A model for cathodic blister growth in coating degradation using mesomechanics approach

M. H. Nazir*, Z. A. Khan, A Saeed and K. Stokes

The paper presents a novel theoretical model of blistering initiation and propagation especially useful for coating life assessment. The focus is on initially circular blisters. A two-part theoretical analysis of blistering is conducted using mesomechanics approach coupling diffusion concepts with fracture mechanics concepts. The diffusion concept is used to treat the corrosive species transport, eventually causing corrosion and blistering, while the fracture mechanics concept is used to treat the blister growth as circular crack propagation. Effects of thickness ratio and modulus ratio on blistering propagation are discussed. A simple criterion is identified which excludes the possibility of widespread blister propagation. Furthermore, a comparative study with the existing blistering models is carried out. Experiments are reported for blistering using a model coating-substrate system, chosen to allow visualisation of interface and to permit coupled (diffusion and residual) stresses in the coating over a full range of interest. The predicted limits from theoretical model are expected to be useful for the manufacturers in the design and deposition of coatings.

1 Introduction

In this research, the focus is on stress-strength model particularly useful for predicting time-dependent degradation and failure of coatings [1]. A number of papers have been published on the degradation of systems exposed to outdoor weathering conditions [2–5]. These models relate the degradation to environmental factors, such as weather using the time series modelling for predicting the daily degradation. Physically, among the degradation parameters, the coating-substrate adhesion is one of the most critical parameters which has been analysed using various modelling techniques [5–7]. One such latest model addressing the effect of variable environmental parameters on coating-substrate adhesion is presented in Ref. [8], which is further utilised in evaluating the life assessment, taking blister formation and growth as a symptom of coating failure.

Despite of great advances in coating technology, blistering still remains one of the serious problems and important parameters [9–13]. It is, therefore, essential to understand the physical and metallurgical phenomenon of blistering from both scientific and engineering point of view. One of the most severe forms of blistering is known as cathodic blistering [14–16], which takes place when a metallic substrate with coating defects is exposed to saline environment, such as salt spray or immersion in salt solution [17–21].

This work is the continuation of research within [7,8,22–29] and aims to develop equations for blistering growth using the concept of mesomechanics of a bilayer composite [30]. Mesomechanics seeks to apply the mechanics principles to the microstructural constituents of materials [31]. The developed equations are then compared with the existing blistering models [15,32–37], since the pioneering work of *Hutchinson* et al. [38]. These models are presented in Table 1. The novelty in this research lies in modelling the blister propagation as a circular symmetric interfacial defect incorporating blister height, which was not analysed in detail in previous blistering models. The diffusion concept is used to treat the corrosive species transport, eventually causing corrosion and blistering, while the fracture mechanics concept is used to treat the blister growth as circular crack propagation. The novel equations are expected to prove beneficent in coating development as well as in prognostics to evaluate the remaining useful life of a coating-substrate systems [39].

M. H. Nazir, Z. A. Khan, A Saeed
Faculty of Science and Technology, Sustainable Design Research Centre (SDRC), Bournemouth University, Bournemouth, Dorset BH9 1JQ (United Kingdom)
E-mail: hnazir@bournemouth.ac.uk
K. Stokes
Defence Science and Technology Laboratory (DSTL), Salisbury (United Kingdom)

Table 1. Available blistering models that can be used for blister initial and propagation

Model	Developer	Reference
$\frac{\alpha^2 \cdot E^2 \delta}{(1-v_c^2)}\left(a_{11}^2 \cdot p_y^2 + 2a_{12}p_x p_y + a_{11}^2 p_x^2\right)$	*Prawoto*	[15]
$\frac{p \cdot \delta\sqrt{1-v_c^2}}{2f}$, where f is the constant dependent on geometry	*Volinsky*	[32]
$\frac{p\sqrt{(1-v_c^2)}}{2\delta}$	*Jahnsen*	[33]
$\left(\frac{p^4 r^4 E^5}{17.4h}\right)^{\frac{1}{6}}$ where h is the coating thickness	*Kappes*	[34]
$\sqrt{p \cdot C \cdot \delta \cdot E}$, where C is constant which depends on the geometry	*Galindo*	[35]
$\frac{p\sqrt{(1-v_c^2)^h}}{2}$, where h is thickness of coating	*Bresser*	[36]
$\frac{E}{2}\sqrt{5 \cdot C \cdot p \cdot \delta}$, where C is the constant which depends on geometry	*Wan*	[37]

In above equations, p is the blister pressure; δ is the blister height; h is coating thickness; E is Young's modulus; r is the blister radius.

2 Preliminary knowledge and experimentation

Blisters are local coating defects that form dome-shaped projections in the coating through local loss of coating-substrate adhesion at constant rate. Cathodic blistering initiation is always associated with some form of defects, such as flaws (micro voids) at the interface between coating and substrate. These interfacial defects allow the transport of corrosive species from the environment to the substrate, where corrosion reaction will take place at the metallic substrate surface, at and around the defects. Corrosion products formed by cathodic reactions (at cathodic sites) reduce the coating-substrate adhesion eventually forming blisters. These cathodic sites are formed within the vicinity of defect along the coating–substrate interface.

The mechanism of blister initiation is based on the disbonding of coating in the presence of diffusion-induced stress at the delamination (crack) front [40,41]. The diffusion of corrosive species introduces diffusion-induced stress in the coating. The driving force leading to blister propagation is the applied bending moment induced by in-plane compressive stress due to temperature change coupled with diffusion-induced stress. In this research, the governing differential equation for internal coupling stresses effecting the blister initiation is derived by considering the coating-substrate system as a bilayer cantilever beam. Then, the fracture equation for the propagation of blister in an axisymmetric circular pattern is derived by using the concepts of von Karman non-linear plate theory [42–47].

In an attempt to illustrate the blister initiation and propagation, the primer-coated steel sample was cooled from fabrication temperature to a lower reference temperature. When the sample was cooled, it bent under the action of residual stresses induced due to mismatch in thermal expansion between coating and substrate. The curvature was measured by using optical interferometry and was used to deduce the residual stress. Then to analyse the effect of diffusion-induced stress due to diffusion in the presence of residual stresses, the sample was tested using compound corrosion testing (CCT) where CCT was performed by strictly maintaining the reference temperature. The test consists of 20 min immersion in 5% NaCl and 11.5 h dry off periods. The total test was 60 cycles and the events were recorded by camera images. The images in Table 2 show the condition of blistering at various cycles. The blisters initiated at 20 cycles of CCT and started to grow at much faster rate and larger at 60 cycles of CCT. Figure 1 shows the summary of the results using cross section of blistering. The figure shows that electrolyte solution penetrates inside the coating towards the interface, where there are defects (micro voids) (Fig. 1a). Once the electrolyte penetrates, certain cathodic reaction sites develop where the coating starts to debond from substrate (Fig. 1b). When the debonded area reaches a critical size, the coating completely delaminates resulting in the formation of nearly circular blister (Fig. 1c). After the blister has formed, it starts to expand in circular manner due to increase in its radius r.

3 Analytical approach

3.1 Basic concept

Before putting into service, the coating-substrate system is pre-cured at elevated temperatures, e.g., 70 °C, introducing tensile in-plane residual stress in the coating. The tension can be as high as 15 MPa [48]. When the coated steel panel is exposed to water solution containing salt, gradual diffusion of water into the coating takes place, eventually causing swelling with volume expansion. The transport of corrosive species introduces diffusion-induced stress in the coating, high enough, that can change the residual stress from 15 MPa tension to 5 MPa compression [49]. During exposure, randomly distributed pores are formed in the coating which provides the conductive pathways for the corrosive species to reach the metal surface. Once the species arrives at the metal surface, an electrochemical corrosion cell is formed, where steel is oxidised at anodes while oxygen is reduced at cathodes. The produced hydroxyl ions at the cathode cause the disbonding of the coating from the substrate and forming corrosion products. The cathodic disbonding, upon reaching the critical size, results in the complete delamination of the coating from the substrate resulting in the formation of blister. The blister propagates

Table 2. The images showing the condition of blistering at various cycles of compound corrosion testing (CCT)

Brand new-coated sample

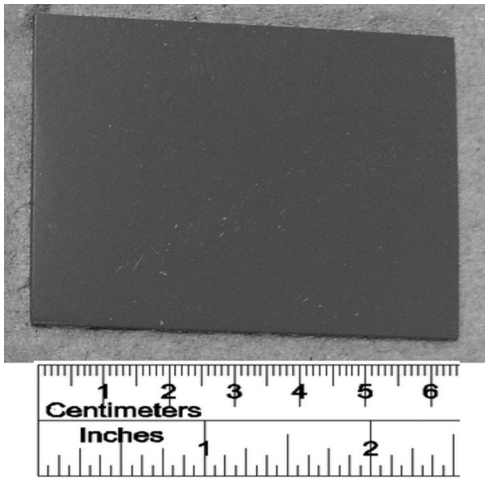

Twenty cycles of CCT, blistering started to appear

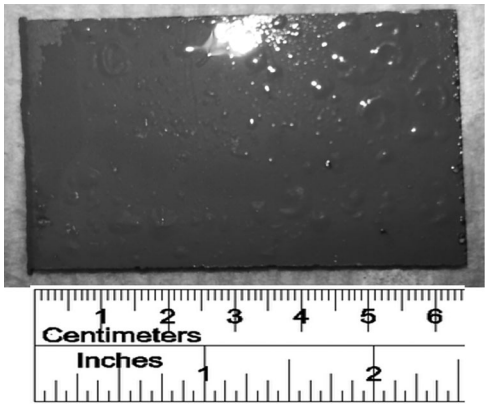

Sixty cycles of CCT, blistering growing faster and larger

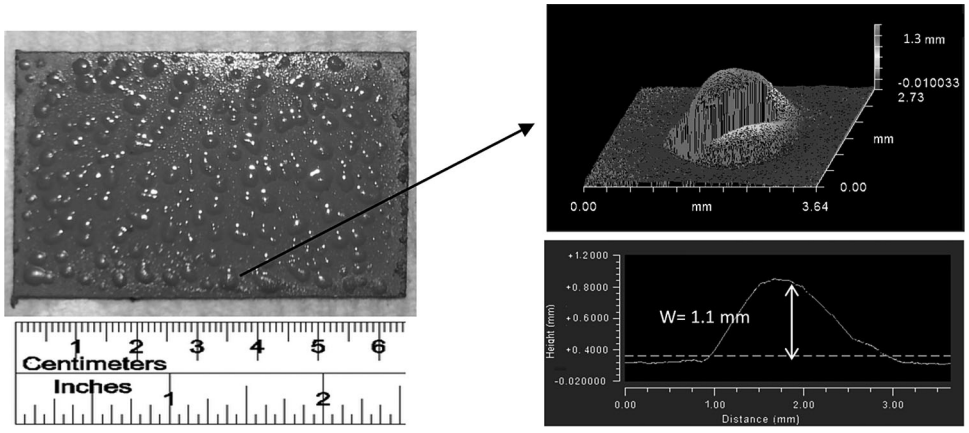

initially in axisymmetric circular pattern and eventually resulting in non-axisymmetric perturbation of crack front producing telephone-cord blister. The focus is initially on propagation in axisymmetric circular pattern; non-axisymmetric unstable propagation will be discussed in future research.

The aim of this research is to develop an analytical model of the circular blistering propagation considering the coupling effects of residual and diffusion-induced stresses. Figure 2 shows two approaches utilised in this research.

3.2 Diffusion concept of blistering

Consider the case of an inhomogeneous distribution of corrosive species in a dilute electrolyte solution. The diffusion of corrosive

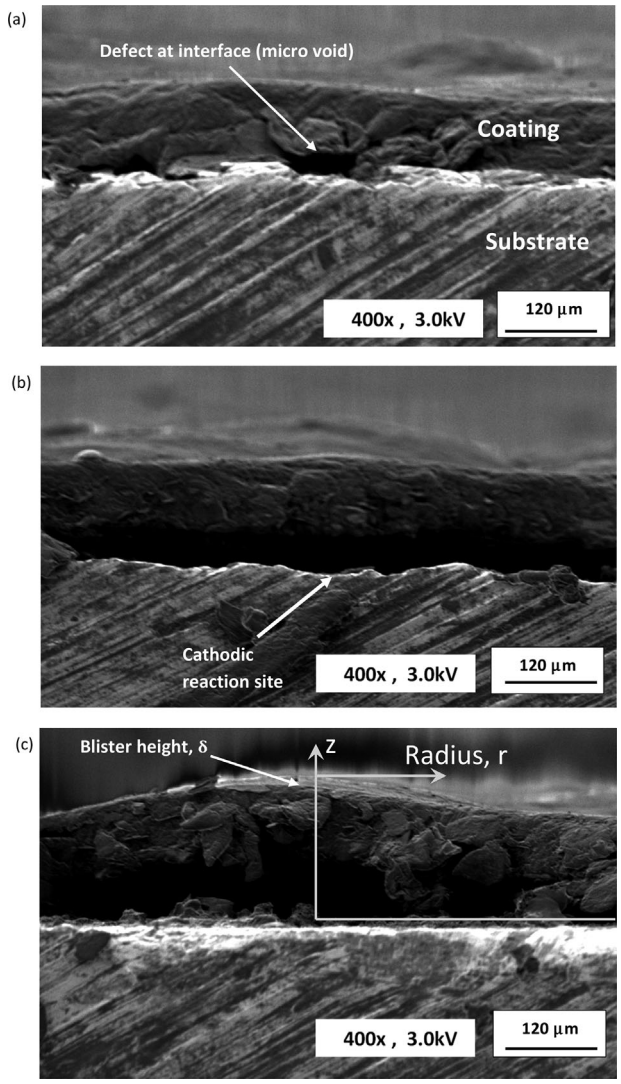

Figure 1. The summary of the experimental results using cross section of blistering; (a) new sample with defect (micro void) at the interface; (b) cathodic reaction site where the coating starts to debond from substrate; (c) formation of circular blister

species k in a stressed elastic solid is associated with principle stresses as [50–53],

$$\frac{\partial c_k}{\partial t} = \vec{\nabla}.\left\{\frac{D_k c_k}{RT}\left[\mu_k - \int_0^{\sigma_i} \bar{V}_k d\left(\frac{1}{3}\int_{i=1}^{i=3}\sigma_i\right)\right]\right\} \quad (1)$$

where c_k is the concentration of corrosive species k in an infinitely dilute electrolyte solution; D_k is the diffusion co-efficient of corrosive species k; R is the molar gas constant and T is temperature; μ_k is the chemical potential of corrosive species k; σ_i are the principle stresses equal to the sum of principle diffusion-induced stresses σ_{d_i} and principle residual stresses σ_{r_i}, i.e., $\sigma_i = \sigma_{r_i} + \sigma_{d_i}$; $\overline{V_k}$ is the scaler term (does not include stress tensor effect) representing the partial molar volume of diffusing corrosive species k.

Consider the above elastic solid as a bilayer cantilever beam with one layer exposed to diffusing corrosive species which maintains a concentration c_o as shown in Fig. 2. The top layer (also called coating, denoted by c) with thickness h, length l_c and width b_c is bonded to a substrate with thickness s, length l_s and width b_s as shown in Fig. 2. The interface of the coating and the substrate on the co-ordinate system is defined at $x = 0$; the free surface of the coating is located at $x = h$ and the free surface of the substrate is located at $x = -s$. Solution of Equation (1) provides with the diffusion equation for the coating including the coupling effect of residual stress and diffusion-induced stress as,

$$\frac{\partial c_{k_c}}{\partial t} = D_{k_c}\left\{\nabla^2 c_{k_c} - \frac{\overline{V_{k_c}}}{9RT}\vec{\nabla}c_{k_c}\vec{\nabla}[\sigma_{r_c} + \sigma_{d_c}] - \frac{\overline{V_{k_c}}}{9RT}c_{k_c}\nabla^2[\sigma_{r_c} + \sigma_{d_c}]\right\} \quad (2)$$

The equation for residual stress in a bilayer cantilever by *Hseuh* [54] is used to address the residual stress in coating. Residual stress in the coating, due to thermal expansion mismatch is introduced when the coating-substrate system is subjected to temperature change, given as [55],

$$\sigma_{r_c} = E_c\left(\frac{(E_s\alpha_s s + E_c\alpha_c h)\Delta T}{(E_s s + E_c h)} + (x - t_b)\left(\frac{3\left[E_s s^2\left(\frac{(E_s\alpha_s s+E_c\alpha_c h)\Delta T}{(E_s s+E_c h)} - \alpha_s\Delta T\right) - E_c h^2\left(\frac{(E_s\alpha_s s+E_c\alpha_c h)\Delta T}{(E_s s+E_c h)}\right) - \alpha_c\Delta T\right]}{E_s s^2(2s + 3t_b) + E_c h^2(2h - 3t_b)}\right) - \alpha_c\Delta T\right) \quad (3)$$

where E_c, E_s and α_c, α_s represent elastic moduli and co-efficient of thermal expansion of the coating and the substrate, respectively; T is temperature change from fabrication temperature or during application; $t_b = \frac{-E_s s^2 + E_c h^2}{2(E_s s + E_c h)}$ defines the bending axis location corresponding to bending strain component being zero; $x = t_b$ dictates the location of neutral axis corresponding to zero strain.

The equation for diffusion-induced normal stress in a bilayer cantilever beam by *Zhang* et al. [56] is used to address the diffusion-induced stress in the coating. The diffusion of corrosive species k at time $t > 0$ will introduce the diffusion-induced stress in the coating, given as,

$$\sigma_{d_c} = E_c\left(\frac{E_c h\, V_{k_c} c_{k_c} + E_s s\ V_{k_s}\ c_{k_s}}{3(E_c h + E_s s)} + (x - t_b)\left(\frac{2[E_c E_s hs(h + s)(V_{k_c}\ c_{k_c} - V_{k_s}\ c_{k_s})]}{E_c^2 h^4 + E_s^2 s^4 + 2E_c E_s hs(2h^2 + 3hs + 2s^2)}\right) - \frac{1}{3}c_{k_c}\ V_{k_c}\right) \quad (4)$$

where, c_{k_c}, c_{k_s} and V_{k_c}, V_{k_s} represent the concentration and partial molar volume of diffusing corrosive species in the coating and the substrate, respectively. Substituting Equations (3) and (4) into Equation (2) gives the solution for coating deformation including the coupling effect of residual stress and diffusion-

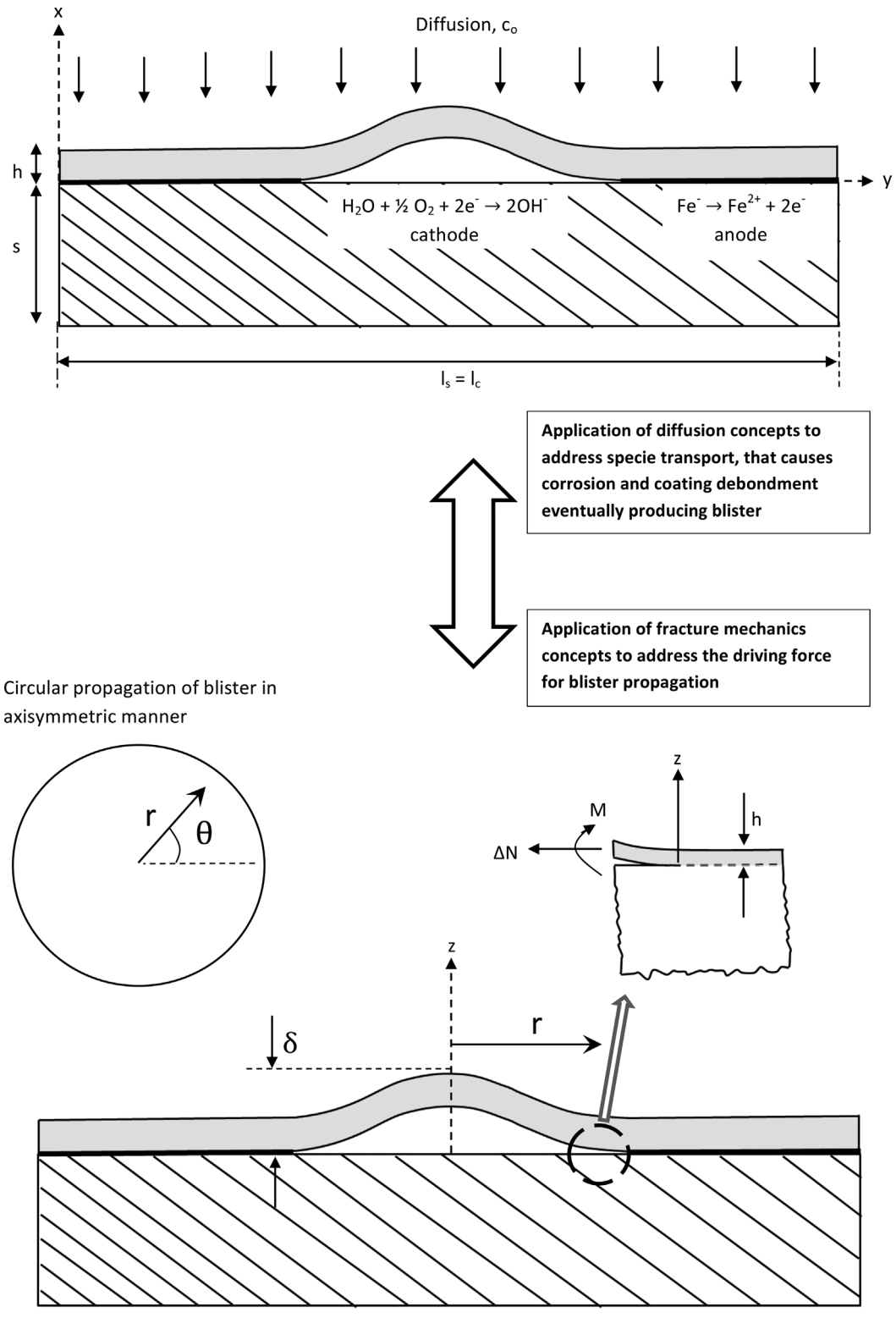

Figure 2. Two approach models of blistering with diffusion concept (upper) coupled with fracture mechanics concept (lower)

induced stress as,

$$\frac{\partial c_{k_c}}{\partial t} = D_{k_c}\left\{\left(1+\frac{E_c\ {V_{k_c}}^2}{9RT}c_{k_c}\right)\frac{\partial^2 c_{k_c}}{\partial x^2}+\frac{E_c {V_{k_c}}^2}{9RT}\left(\frac{\partial c_{k_c}}{\partial x}\right)^2 - \frac{{V_{k_c}}^2}{9RT}\frac{\partial c_{k_c}}{\partial x}\left(\frac{\partial \sigma_{r_c}}{\partial x}+\frac{\partial \sigma_{d_c}}{\partial t}\right)\right\} \quad (5)$$

The effect of residual stress and concentration of diffusing corrosive species on feed-back diffusion-induced stress can be found by solving Equation (5) as,

$$\sigma'_d = \frac{\partial \sigma_{d_c}}{\partial t} = \frac{\left(9RT + E_c + {V_{k_c}}^2 c_{k_c}\right)\frac{\partial^2 c_{k_c}}{\partial x^2} + E_c {V_{k_c}}^2\left(\frac{\partial c_{k_c}}{dx}\right)^2 - \frac{\partial c_{k_c}}{\partial t}\frac{9RT}{D_{k_c}}}{{V_{k_c}}^2\frac{\partial c_{k_c}}{\partial x}} - \frac{\partial \sigma_{r_c}}{\partial x} \quad (6)$$

The feed-back diffusion-induced stress can either be uniform state of equi bi-axial compression or tension depending upon the concentration of diffusing corrosive species c_{k_c} and direction of residual stress gradient $\partial\sigma_{r_c}/\partial x$. When under compression, the coating at cathodic sites debonds from the substrate, which upon reaching the critical size results in the formation of blister. Given a stress tensor σ, the pressure p in terms of hoop stress is defined as $p = h\sigma/r$ [57]; therefore Equation (6) can be modified in terms of pressure as,

$$p_d = \frac{h}{r}\left[\frac{\left(9RT + E_c {V_{k_c}}^2 c_{k_c}\right)\frac{\partial^2 c_{k_c}}{\partial x^2} + E_c {V_{k_c}}^2\left(\frac{\partial c_{k_c}}{\partial x}\right)^2 - \frac{\partial c_{k_c}}{\partial t}\frac{9RT}{D_{k_c}}}{{V_{k_c}}^2\frac{\partial c_{k_c}}{\partial x}} - \frac{\partial \sigma_{r_c}}{\partial x}\right] \quad (7)$$

where, p_d is the feed-back diffusion-induced pressure at a point inside the blister cavity.

3.3 Fracture mechanics concept of blistering

While the previous section discusses about the diffusion of corrosive species, this section discusses the effect of feed-back diffusion-induced pressure p_d on blister propagation using the concepts of von Karman non-linear plate theory within the frame work of fracture mechanics. With reference to the schematic in Fig. 2, consider a blister of radius r. An interface crack with axisymmetric circular shape exists between the coating and the substrate such that when the coating is intact (blister height, $\delta = 0$), the feed-back diffusion-induced stress σ'_d is a uniform state of equi bi-axial compression $\left(\sigma_d = \sigma_d = -\sigma'_d\right)$. In the intact state, the stress intensity factors and elastic energy release rate of interface crack are zero. Only when the coating debonds from the substrate, is the case of non-zero crack driving force.

Consider the case when $r/h >> 1$, the disbonding of the coating is modelled as a completely intact circular plate using von Karman non-linear plate theory. The intact plate debonds in a stable axisymmetric circular pattern when normalised pressure $p/p_{cr} > 1$. The conventional form of normalised stress ($\frac{\sigma}{\sigma_{cr}} = \frac{(1-\nu_c^2)}{E_c}\sigma\left(\frac{r}{h}\right)^2$ [38]), can now be modified in terms of normalised feed-back diffusion-induced pressure by incorporating Equation (7) as,

$$\frac{p_d}{p_{cr}} = \frac{(1-\nu_c^2)}{E_c}\left[\frac{\left(9RT + E_c\ {V_{k_c}}^2 c_{k_c}\right)\frac{\partial^2 c_{k_c}}{\partial x^2} + E_c {V_{k_c}}^2\left(\frac{\partial c_{k_c}}{\partial x}\right)^2 - \frac{\partial c_{k_c}}{\partial t}\frac{9RT}{D_{k_c}}}{{V_{k_c}}^2\frac{\partial c_{k_c}}{\partial x}} - \frac{\partial \sigma_{r_c}}{\partial x}\right]\left(\frac{r}{h}\right)^3 \quad (8)$$

where p_d/p_{cr} can increase due to either increase in blister radius r or to an increase in feed-back diffusion-induced pressure p_d.

The mode adjusted driving force F for crack propagation depends on the elastic energy release rate G and a dimensionless mode mix function $f(\psi)$[58],

$$F = \frac{G}{f(\psi)} \quad (9)$$

where

$$G = \frac{6\left(1-\nu_c^2\right)}{E_c h^3}\left[M_c^2 + \frac{1}{12}h^2\Delta N^2\right] \quad (9(a))$$

$$f(\psi) = sec^2[(1-\lambda)\psi] \quad (9(b))$$

$$\psi = \frac{K_2}{K_1} = cot\frac{\cos\ \omega + \left[\frac{h\Delta N}{\sqrt{12}M_c}\right]\sin\omega}{\left[\frac{h\Delta N}{\sqrt{12}Mc}\right]\cos\omega - \sin\omega} \quad (9(c))$$

$$h\Delta N/\sqrt{12}M_c = 0.2(1+\nu_c)\left(\frac{\delta}{h}\right) \quad (9(d))$$

$$\frac{\delta}{h} = \sqrt{\left(\frac{1}{0.2(1+\nu_c)+0.2\left(1-\nu_c^2\right)}\left(\frac{p_d}{p_{cr}}-1\right)\right)} \quad (9(e))$$

where ψ is a parameter defining mode II to mode I ratio of crack edge; λ is the material parameter and best fit λ is found to be about 0.2 for primer-coated steel sample [59]; M_c is the bending moment of the crack edge of coating; N is the resultant stress force acting on the coating; parameter ω in Equation (9(c)) is dependent upon Dundur's elastic mismatch parameter χ [60], where $\chi = \left(\overline{E_c} - \overline{E_s}\right)/\left(\overline{E_c} + \overline{E_s}\right)$ [61].

From Equation (9(a)–c)), it can be seen that G, $f(\psi)$ and ψ at the edge of crack depend on the combination $h\Delta N/\sqrt{12}M_c$ in Equation (9(d)), the term being the function of normalised feed-back diffusion-induced pressure p_d/p_{cr}. After substitutions, Hutchinson's equations for G, $f(\psi)$ and ψ can be modified to

redefine the interfacial crack propagation problem in terms of feed-back diffusion-induced pressure.

The condition for the incipient fracture propagation is $F = IC$ [62], where IC is mode I toughness. By incorporating feed-back diffusion-induced pressure p_d and incipient condition $F = IC$, it is possible to find the incipient spread of circular blister as [62],

$$\sqrt{\frac{G_o}{F}} = (1 - v_c)h = p_d\sqrt{\left[\frac{(1 - v_c)h}{E_{cIC}}\right]};\ \ G_o = p_d^2\frac{(1 - v_c)h}{E_c} \tag{10}$$

The left-hand side of the equation is a function of p_d/p_{cr}; the equation is used to generate curves for incipient spread of circular blister. Equation (10) also benefits in making the theoretical predictions for coating failure due to blistering.

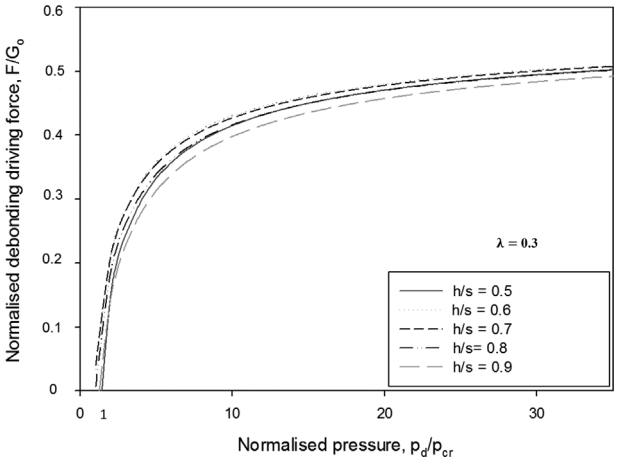

Figure 4. The effects of plots of normalised feed-back diffusion-induced pressure on normalised (mode adjusted) debonding driving force

4 Results and discussion

Based on numerical simulations, blister growth and propagation as a circular symmetric interfacial defect are discussed in this section.

To illustrate the effects of normalised feed-back diffusion-induced pressure on normalised blister height, comparisons of the predicted blister height from previous blistering models are first carried out and shown in Fig. 3. The rising plot for the predicted blister height is in agreement with the previously reported models, however, conventional models except *Prawoto* et al. [15] did not include the horizontal circular propagation of blister, instead they only modelled the vertical growth of blister height. Nevertheless, both the horizontal and vertical progression of blister is important to be modelled in order to completely understand the mechanism of blistering.

The effects of plots of normalised feed-back diffusion-induced pressure on normalised (mode adjusted) disbonding driving force are shown in Fig. 4. The plots show that above a certain value of p_d/p_{cr}, the disbonding driving force F diminishes with increasing p_d/p_{cr}, considering $\lambda = 0.3$. Therefore, a growing circular blister, in a state to the right of maxima is stable and grows in an axisymmetric circular pattern. The plots in Fig. 4 also show that the effect of thickness ratio h/s on disbonding driving force is negligible, which indicates that increasing the coating thickness, is not necessarily an effective method for achieving the better performance of the coating while combating blistering. Figure 5 shows the evolution of disbonding driving force to various modulus ratio E_s/E_c. The plots in Fig. 5 show that the disbonding driving force increases with decreasing the modulus ratio. This indicates that for a given coating thickness, the coating flexibility can decrease the disbonding driving force, and thereby improve the performance of the coating in terms of blistering.

A better plot revealing the parameters controlling the blister propagation are obtained by simulating Equation (10) as shown in Fig. 6. For the purpose of discussion, focus on the trend for h/s = 0.9 in Fig. 6. Consider the case of coating thickness h being fixed and the initial circular defect (micro void) exists at the

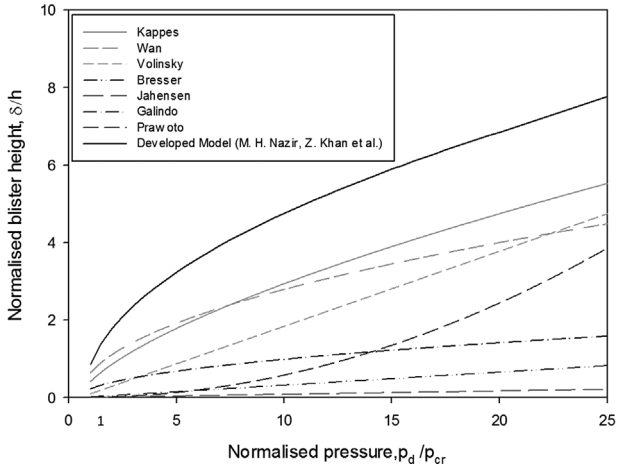

Figure 3. Comparison of the predicted blister height from previous blistering models with the developed model

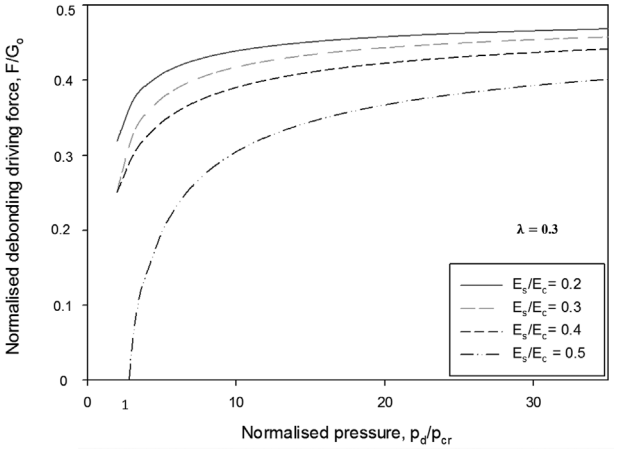

Figure 5. The evolution of debonding driving force to various modulus ratio

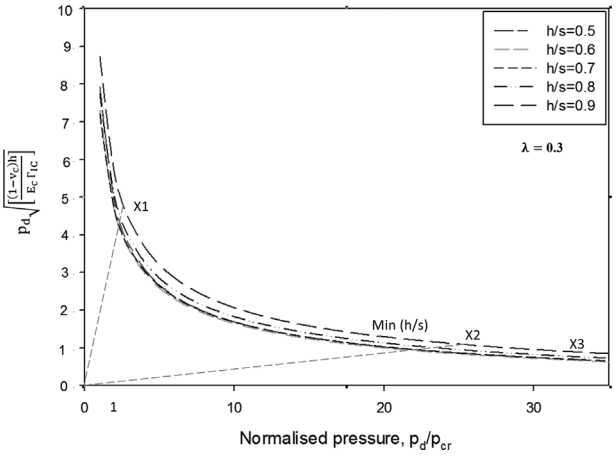

Figure 6. Normalised pressure associated with incipient propagation of circular blister for various values of thickness ratio

interface with the coating loaded by increasing p_d. The loading corresponds to the straight line trajectory in Fig. 6. If the blistering parameters are such that the straight line trajectory is one like OX1, which crosses the trend to the left of minima, than the blister will experience an unstable propagation until it is arrested at X3. With further increase in p_d, the blister propagates in a stable circular manner. However, if the straight line trajectory is one like OX2, crossing the trend at the right of minima, than the blister will be stable right from the initiation. The plots in Fig. 6 also show that the incipient propagation of circular blister is independent of the coating thickness.

The plots in Fig. 7 show that the incipient propagation of circular blister is not much influenced by the modulus ratio. For every value of modulus ratio in Fig. 7, the incipient blister propagation will become stable at same minima corresponding to $p_d/p_{cr} = 20$. Let Min (h/s) denotes the minima of the propagation trends in Fig. 7 for a given thickness ratio h/s. There will be no blister propagation irrespective of the size of initial defect (micro void), if $p_d\sqrt{\left[\frac{(1-\nu_c)h}{E_c\,\Gamma_{IC}}\right]} < \text{Min (h/s)}$. The threshold is useful for the manufacturers in design and

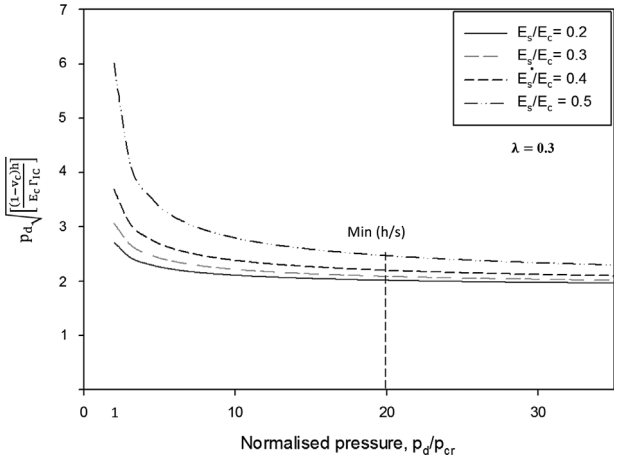

Figure 7. The incipient propagation of circular blister for various values of modulus ratio

durability of coatings, as it guarantees that the extensive propagation of delamination will not occur, nonetheless as circular blisters. It is worth noting that the minima in Figs. 6 and 7 are attained at $p_d/p_{cr} = 20$, which fosters an important explanation of small interfacial defect as the one which satisfies the condition $r \ll \left(r^* = h\left[\frac{(1-\nu_c)E_c h}{\left(\min^2\left(1-\nu_c^2\right)^2\Gamma_{IC}\right)^{\frac{1}{4}}}\right]\right)$. For the case when initial interfacial defect is analogous to r^*, than there will be no blister propagation until r greatly exceeds from r^*.

5 Conclusions

A two-part theoretical model for blistering is developed using mesomechanics approach coupling the diffusion concepts with fracture mechanics concepts. An initial calculation developed the diffusion equation for blistering considering coating-substrate system as a bilayer cantilever beam. The diffusion of corrosive species introduces diffusion-induced stress in the coating which is coupled with in-plane compressive stress due to temperature change. A second calculation produced the fracture equation for the propagation of blister in an axisymmetric circular pattern by using the von Karman non-linear plate theory. Equation (8) is the diffusion equation, which combined with fracture Equation (9), provides the relationship between the blister initiation due to diffusion of corrosive species and propagation of blister as a circular interfacial crack.

Results indicate that the blister propagation is independent of thickness ratio h/s, however, higher modulus ratio E_s/E_c can significantly improve the performance of coating in terms of blistering. A simple criterion is identified as Min (h/s) on the prediction curves for blister propagation; if the parameters are such that the blister propagation is less than minima than there will be no blister growth which excludes the possibility of widespread blister propagation. However, for the case when blister propagation corresponding to parameters is greater than minima than the blister will propagate in a stable circular pattern. The developed theoretical model, with slight additions can be used for predicting the instabilities of circular blister, forming "telephone cord blister" which will be discussed in the future work as a continuation of this work.

Acknowledgements: This research is joint funded by Defence Science and Technology Laboratory (DSTL), Ministry of Defence (MoD) and Bournemouth University UK. The authors acknowledge their support and contributions.

6 References

[1] S. Kotz, Y. Lumelskii, M. Pensky, *Theory and Applications*, World Scientific, Singapore **2003**, p. 44.
[2] V. Chan, W. Q. Meeker, *Estimation of Degradation-Based Reliability in Outdoor Environments, Technical Report*, Iowa State University, Ames **2001**.
[3] A. Heutink, A. Van Beek, J. Van Noortwijk, H. Klatter, A. Barendregt, *XXVII FATIPEC Congress, 19–21 April 2004*, Aix-en-Provence, France, AFTPVA, Paris **2004**, pp. 351–364.

[4] J. Van Noortwijk, *Reliab. Eng. Syst. Safe.* **2009**, *94*, 2–21.
[5] R. P. Nicolai, R. Dekker, J. M. van Noortwijk, *Reliab. Eng. Syst. Safe.* **2007**, *92*, 1635.
[6] K. L. Mittal, *Adhesion Aspects of Polymeric Coatings*, Springer Science & Business Media, New York, USA **2012**.
[7] M. Nazir, Z. A. Khan, K. Stokes, *J. Adhes. Sci. Technol.* **2015**, *29*, 1415.
[8] M. H. Nazir, Z. Khan, K. Stokes, *J. Adhes. Sci. Technol.* **2015**, *29*, 392.
[9] J. Meneve, K. Vercammen, E. Dekempeneer, J. Smeets, *Surf. Coat. Technol.* **1997**, *94*, 476.
[10] A. Matthews, A. Leyland, *Surf. Coat. Technol.* **1995**, *71*, 88.
[11] K. Holmberg, A. Mathews, *Thin Solid Films* **1994**, *253*, 173.
[12] M. Subanovic, D. Naumenko, M. Kamruddin, G. Meier, L. Singheiser, W. Quadakkers, *Corros. Sci.*, **2009**, *51*, 446.
[13] C. Courcier, V. Maurel, L. Rémy, S. Quilici, I. Rouzou, A. Phelippeau, *Surf. Coat. Technol.* **2011**, *205*, 3763.
[14] T. N. Nguyen, J. B. Hubbard, G. B. McFadden, *J. Coat. Technol.* **1991**, *63*, 43.
[15] Y. Prawoto, B. Dillon, *J. Fail. Anal. Prevent.* **2012**, *12*, 190.
[16] M. H. Nazir, Z. A. Khan, K. Stokes, *J. Adhes. Sci. Technol.* **2015**, *29*, 1200.
[17] D. Rickerby, S. Bull, *Surf. Coat. Technol.* **1989**, *39*, 315.
[18] V. Raja, R. G. Devi, A. Venugopal, N. Debnath, J. Giridhar, *Surf. Coat. Technol.* **1998**, *107*, 1.
[19] H. Bi, J. Sykes, *Corros. Sci.* **2011**, *53*, 3416.
[20] Y. Prawoto, I. H. Onn, *Comput. Mater. Sci.* **2012**, *62*, 105.
[21] I. Alig, M. Bargmann, H. Oehler, D. Lellinger, M. Wanner, D. Koch, *J. Phys. D: Appl. Phys.* **2011**, *44*, 034009.
[22] Z. A. Khan, M. Grover, M. H. Nazir, *Transactions on Engineering Technologies*, Springer, Berlin, New York **2015**, pp. 413–423.
[23] M. H. Nazir, Z. A. Khan, *International Journal of Computational Methods & Experimental Measurements*, WIT Press, Southampton, **2015**.
[24] A. Saeed, Z. Khan, M. Clark, M. Nel, R. Smith, *Insight Non Destr Test. Cond. Monit.* **2011**, *53*, 382.
[25] A. Saeed, Z. A. Khan, M. Hadfield, S. Davies, *Tribol. T.* **2013**, *56*, 637.
[26] A. Saeed, Z. A. Khan, E. Montgomery, *Mater. Perform. Charact.* **2013**, *2*, 1.
[27] Z. A. Khan, P. Pashaei, R. S. Bajwa, M. H. Nazir, M. Camak, *International Journal of Computational Methods & Experimental Measurements*, WIT Press, Southampton **2015**.
[28] M. H. Nazir, Z. A. Khan, K. Stokes, *J. Adhes. Sci. Technol.* **2015**, *29*, 1415.
[29] M. H. Nazir, Z. A. Khan, A. Saeed, R. S. Bajwa, K. Stokes, *Corrosion*, NACE, Houston, Texas **2015** (in press).
[30] V. Panin, T. Elsukova, Y. F. Popkova, *Dokl. Phys.* **2012**, *57*, 100.
[31] Y. Prawoto, *Solid Mechanics for Materials Engineers-Principles and Applications of Mesomechanics*, Lulu.com, Morrisville NC, USA **2013**.
[32] A. Volinsky, N. Moody, W. Gerberich, *Acta Mater.* **2002**, *50*, 441.
[33] H. Jahnsen, *Handbook of Materials Behavior Models*, Academic Press, Waltham **2001**, p. 582.
[34] M. Kappes, G. Frankel, N. Sridhar, *Prog. Org. Coat.* **2010**, *69*, 57.
[35] R. E. Galindo, A. Van Veen, J. Evans, H. Schut, J. T. M. De Hosson, *Thin Solid Films* **2005**, *471*, 170.
[36] J. Bressers, S. Peteves, M. Steen, *Eur. Struct. Integrity Soc.* **2000**, *26*, 115.
[37] K.-t. Wan, K. Liao, *Thin Solid Films* **1999**, *352*, 167.
[38] J. Hutchinson, M. Thouless, E. Liniger, *Acta Metall. Mater.* **1992**, *40*, 295.
[39] D. Brown, D. Darr, J. Morse, B. Laskowski, in: *Annual Conference of the Prognostics and Health Management Society*, **2012**, pp. 1–12.
[40] T. Chuang, T. Nguyen, S. Li, in: *Damage and Failure of Interfaces. 1st International Conference*. Proceedings, **1997**, pp. 203–209.
[41] R. Souto, Y. González-García, S. González, *Prog. Org. Coat.* **2009**, *65*, 435.
[42] J. Reddy, *Int. J. Solid. Struct.* **1984**, *20*, 881.
[43] L. B. Freund, S. Suresh, *Thin Film Materials: Stress, Defect Formation and Surface Evolution*: Cambridge University Press, Cambridge **2004**.
[44] B. Audoly, *Phys. Rev. Lett.*, **1999**, *83*, 4124.
[45] Z. Chen, B. Cotterell, W. Wang, E. Guenther, S.-J. Chua, *Thin Solid Films* **2001**, *394*, 201.
[46] M.-W. Moon, K.-R. Lee, K.-H. Oh, J. W. Hutchinson, *Acta Mater.* **2004**, *52*, 3151.
[47] M. Zhao, J. Zhou, F. Yang, T. Liu, T.-Y. Zhang, *Eng. Fract. Mech.* **2007**, *74*, 2334.
[48] T. Nguyen, J. Hubbard, J. Pommersheim, *J. Coat. Technol.* **1996**, *68*, 45.
[49] T.-J. Chuang, T. Nguyen, S. Lee, *J. Coat. Technol.* **1999**, *71*, 75.
[50] F. Yang, J. Li, *J. Appl. Phys.* **2003**, *93*, 9304.
[51] B. P. Van Milligen, P. Bons, B. A. Carreras, R. Sánchez, *Eur. J. Phys.* **2005**, *26*, 913.
[52] F.-Z. Xuan, S.-S. Shao, Z. Wang, S.-T. Tu, *Thin Solid Films* **2010**, *518*, 4345.
[53] Y. Prawoto, *Mater. Corros.* **2013**, *64*, 794.
[54] C.-H. Hsueh, *J. Appl. Phys.* **2002**, *91*, 9652.
[55] F.-Z. Xuan, L.-Q. Cao, Z. Wang, S.-T. Tu, *Comput. Mater. Sci.* **2010**, *49*, 104.
[56] X. Zhang, W. Shyy, A. M. Sastry, *J. Electrochem. Soc.* **2007**, *154*, A910.
[57] M. J. Buehler, H. Gao, *Nature* **2006**, *439*, 307.
[58] L. Yao, R. Alderliesten, M. Zhao, R. Benedictus, *Compos. Part A: Appl. S. Manuf.* **2014**, *66*, 65.
[59] J. W. Hutchinson, M. Mear, J. R. Rice, *J. Appl. Mech.* **1987**, *54*, 828.
[60] J. W. Hutchinson, *Metal and Ceramic Interfaces, Acta/Scripta Metall. Proceedings Series*, Pergamon, New York **1990**, p. 295.
[61] S. Schmauder, M. Meyer, *Zeitschrift für Metallkunde* **1992**, *83*, 524.
[62] A. G. Evans, D. Mumm, J. Hutchinson, G. Meier, F. Pettit, *Prog. Mater. Sci.* **2001**, *46*, 505.

(Received: July 15, 2015) W8562
(Accepted: October 2, 2015)